

Accelerated Contrast-Enhanced Whole-Heart Coronary MRI Using Low-Dimensional-Structure Self-Learning and Thresholding

Mehmet Akçakaya,¹ Tamer A. Basha,¹ Raymond H. Chan,¹ Hussein Rayatzadeh,¹ Kraig V. Kissinger,¹ Beth Goddu,¹ Lois A. Goepfert,¹ Warren J. Manning,^{1,2} and Reza Nezafat^{1*}

We sought to evaluate the efficacy of prospective random undersampling and low-dimensional-structure self-learning and thresholding reconstruction for highly accelerated contrast-enhanced whole-heart coronary MRI. A prospective random undersampling scheme was implemented using phase ordering to minimize artifacts due to gradient switching and was compared to a randomly undersampled acquisition with no profile ordering. This profile-ordering technique was then used to acquire contrast-enhanced whole-heart coronary MRI in 10 healthy subjects with 4-fold acceleration. Reconstructed images and the acquired zero-filled images were compared for depicted vessel length, vessel sharpness, and subjective image quality on a scale of 1 (poor) to 4 (excellent). In a pilot study, contrast-enhanced whole-heart coronary MRI was also acquired in four patients with suspected coronary artery disease with 3-fold acceleration. The undersampled images were reconstructed using low-dimensional-structure self-learning and thresholding, which showed significant improvement over the zero-filled images in both objective and subjective measures, with an overall score of 3.6 ± 0.5 . Reconstructed images in patients were all diagnostic. Low-dimensional-structure self-learning and thresholding reconstruction allows contrast-enhanced whole-heart coronary MRI with acceleration as high as 4-fold using clinically available five-channel phased-array coil. Magn Reson Med 67:1434–1443, 2012. © 2012 Wiley Periodicals, Inc.

Key words: compressed sensing; accelerated imaging; image reconstruction; LOST; whole-heart coronary MRI; contrast-enhanced

Despite several advances over the last decade, coronary MRI is still faced with major challenges including long scan time, low-signal-to-noise-ratio (SNR), and blood-myocardium contrast-to-noise-ratio (CNR). Several methods have been used to address these limitations. These include application of T_2 magnetization preparation

technique [1,2], more efficient k -space sampling [3,4], administration of vasodilators [5], and imaging at higher magnetic field strengths [6–8]. An alternative method for improving image quality is the use of exogenous contrast agents [9–17]. Administration of T_1 -shortening exogenous contrast agents, via intravascular [9–11] or extracellular [12–17] contrast agents, has been shown to improve coronary MRI. However, conventional gadolinium-based extracellular contrast agents, such as gadopentetate dimeglumine, diffuse to interstitial space quickly. To take advantage of the presence of these contrast media, early studies on coronary MRI were typically performed using breath-hold acquisitions during the first passage of these agents [12,14]. The short acquisition times required for such an approach limits the spatial resolution as well as the coverage required in whole-heart coronary MRI [15–17]. Gadobenate dimeglumine (Gd-BOPTA; MultiHance; Bracco Imaging SpA, Milan, Italy), an extracellular contrast agent with a long plasma half-life, has recently been used to image coronary arteries with improved SNR and CNR [16–18]. To fully take advantage of the presence of contrast media and to reduce imaging artifacts due to contrast agent clearance, while reducing sensitivity to changes in inversion time, a short scan time is desirable.

Non-Cartesian trajectories [19], or parallel imaging techniques such as generalized autocalibrating partially parallel acquisition [16,18] or sensitivity encoding [17,20], have been used in previous studies to reduce the scan time of coronary MRI, with resultant acceleration rates of up to 2-fold while using cardiac-coil arrays with 5–16 elements and higher acceleration rates with 32-channel coils [21,22]. Compressed sensing (CS) is a novel image reconstruction method for accelerated acquisitions with incoherently undersampled k -space data that exploits the sparsity of the image in a transform domain [23,24] and may be used to surpass the current rapid acquisition techniques in terms of acceleration rate [25]. Recently, an improved CS-based reconstruction strategy for incoherently undersampled data, called low-dimensional-structure self-learning and thresholding (LOST), was proposed [26]. However, efficacy of CS-based acceleration for contrast-enhanced coronary MRI has not been investigated.

To demonstrate efficacy of CS for scan time reduction in contrast-enhanced coronary MRI, a truly prospective undersampling data acquisition are needed due to changes in the contrast media in the blood pool that will

¹Department of Medicine, Beth Israel Deaconess Medical Center and Harvard Medical School, Boston, Massachusetts, USA.

²Department of Radiology, Beth Israel Deaconess Medical Center and Harvard Medical School, Boston, Massachusetts, USA.

Grant sponsor: NIH; Grant numbers: R01EB008743-01A2, NIH UL1 RR025758-01; Grant sponsor: Harvard Clinical and Translational Science Center, National Center for Research Resources.

*Correspondence to: Reza Nezafat, PhD, Beth Israel Deaconess Medical Center, 330 Brookline Avenue, Boston, MA 02215, USA. E-mail: rnezafat@bidmc.harvard.edu

Received 15 November 2011; revised 26 January 2012; accepted 13 February 2012.

DOI 10.1002/mrm.24242

Published online 5 March 2012 in Wiley Online Library (wileyonlinelibrary.com).

directly impact image quality. The incoherence requirement of CS techniques is achieved by random undersampling of k -space data. For three-dimensional (3D) coronary MRI with Cartesian sampling, in addition to the random undersampling of lines in $k_y - k_z$ plane, the profile ordering in which these lines are acquired has substantial impact on the imaging contrast and artifacts. Eddy current artifacts from rapid gradient switching that occurs from the profile ordering could have significant impact on image quality [27]. Therefore, to fully use prospective undersampling for contrast-enhanced coronary MRI with CS, the profile-ordering method needs to be changed to be suitable for the randomly undersampled k -space.

In this study, we sought to evaluate the efficacy of prospective random undersampling and LOST reconstruction for highly accelerated contrast-enhanced whole-heart inversion recovery steady state-free precession (SSFP) coronary MRI at 1.5 T, allowing for the better use of the presence of bolus infusion of Gd-BOPTA.

MATERIALS AND METHODS

All imaging sequences were implemented on a 1.5-T Philips Achieva (Philips Healthcare, Best, the Netherlands) system with a five-channel cardiac phased-array receiver coil. For this HIPPA-compliant study, the imaging protocol was approved by our institutional review board, and written informed consent was obtained from all participants.

The study includes two steps. Initially, we implemented and tested a modified radial profile ordering for a randomly undersampled k -space. Both phantom and in vivo experiments were performed to evaluate the proposed ordering scheme. Subsequently, we used this undersampling scheme to acquire highly undersampled contrast-enhanced coronary MRI.

Profile Ordering for Randomly Undersampled k -Space

In our study, an electrocardiogram-triggered, free-breathing, segmented acquisition sequence is used for 3D coronary MRI [17]. In each heartbeat, 20–25 $k_y - k_z$ lines are sampled. For a prospective random undersampling implementation, the $k_y - k_z$ lines are randomly divided into two groups: group A and group B. The center of k -space with a predefined size is included in group A, while the outer region of k -space could belong to either group A or group B. During imaging, the lines in group A are acquired, while the lines in group B are skipped. This achieves an acceleration rate equal to (Total Number of Lines/Number of lines in group A). In segmented acquisition, the lines in group A are divided into different shots, where a *shot* is a group of lines that is acquired in one heartbeat. The division of the lines among different shots and the acquisition order of the lines inside each shot follow a specific profile ordering scheme: first, each line is assigned magnitude and phase values based on its location in $k_y - k_z$ plane [i.e. magnitude = $\sqrt{k_y^2 + k_z^2}$ and phase = $\text{atan}(k_z/k_y)$]. Then, lines are assigned to different shots based on their phase values, such that a line with lower phase value is assigned to an earlier shot during the acquisition. Then, within each shot, lines are sorted based on their magni-

tude values, such that a line with lower magnitude value is acquired first in the shot. The number of lines per shot is usually determined by the turbo imaging factor (i.e. the number of phase encode lines acquired in each heartbeat), which is usually around 20–25 lines per heartbeat. This results in our proposed modified radial acquisition scheme, depicted in Fig. 1a,b, that helps to lower both the number and magnitude of the k -space jumps during the acquisition.

To distinguish between artifacts due to data undersampling when compared with other sources of artifacts such as Eddy currents, two options were incorporated into the imaging pulse sequence: (1) *true undersampling*: the k -space is undersampled with the desired acceleration rate, and the scan completes upon acquiring these lines as depicted in Figs. 1b and (2) *simulated undersampling*: a true undersampling acquisition is performed for a given acceleration rate, followed by the acquisition of the remaining k -space lines to generate a fully sampled k -space, as shown in Fig. 1c.

To evaluate the proposed profile-ordering scheme, a pilot phantom study was conducted. Three sets of images were acquired to demonstrate the artifacts associated with the sampling scheme. A fully sampled reference 3D scan was performed using conventional radial profile ordering in a segmented acquisition using a simulated electrocardiogram. A 3D SSFP imaging sequence with the following parameters was used: TR/TE/ α = 3.8/1.9/110°, FOV = 256 × 256 × 30 mm³, and resolution = 1.3 × 1.3 × 2 mm³. Subsequently, a fully sampled acquisition was performed but with a randomly ordered profile. Finally, a scan was performed using the proposed profile order with an acceleration rate of 2 using the simulated undersampling scheme. To establish the efficacy of the proposed profile ordering for in vivo data, four healthy adult subjects (two females, 20.3 ± 1.5 years) were imaged with a 3D-segmented SSFP sequence using non-contrast-enhanced targeted right coronary MRI protocol [28]. Targeted acquisitions were performed instead of whole-heart acquisitions to allow for multiple acquisitions that can be completed in a reasonable amount of time. Contrast agents were not used to avoid changes due to contrast washout between different datasets. Four imaging datasets were acquired from each subject: (a) a fully sampled reference dataset with conventional radial profile ordering, (b) a fully sampled dataset with a totally random profile order, (c) a 2-fold undersampled dataset with a random undersampling pattern acquired using the modified radial profile order, and (d) a fully sampled dataset with a simulated random undersampling (of rate 2) acquired using the modified radial profile order. For all the scans, the imaging parameters were as follows: TR/TE/ α = 4.3/2.1/90°, FOV = 270 × 270 × 30 mm³, and resolution = 1 × 1 × 3 mm³. The acquired raw data were then transferred to a workstation where LOST reconstruction was performed, as described in the image reconstruction section.

Accelerated Contrast-Enhanced Coronary MRI

Healthy Subject Study

Ten healthy adult subjects (seven females, 30.0 ± 14.8 years) were recruited for contrast-enhanced whole-heart

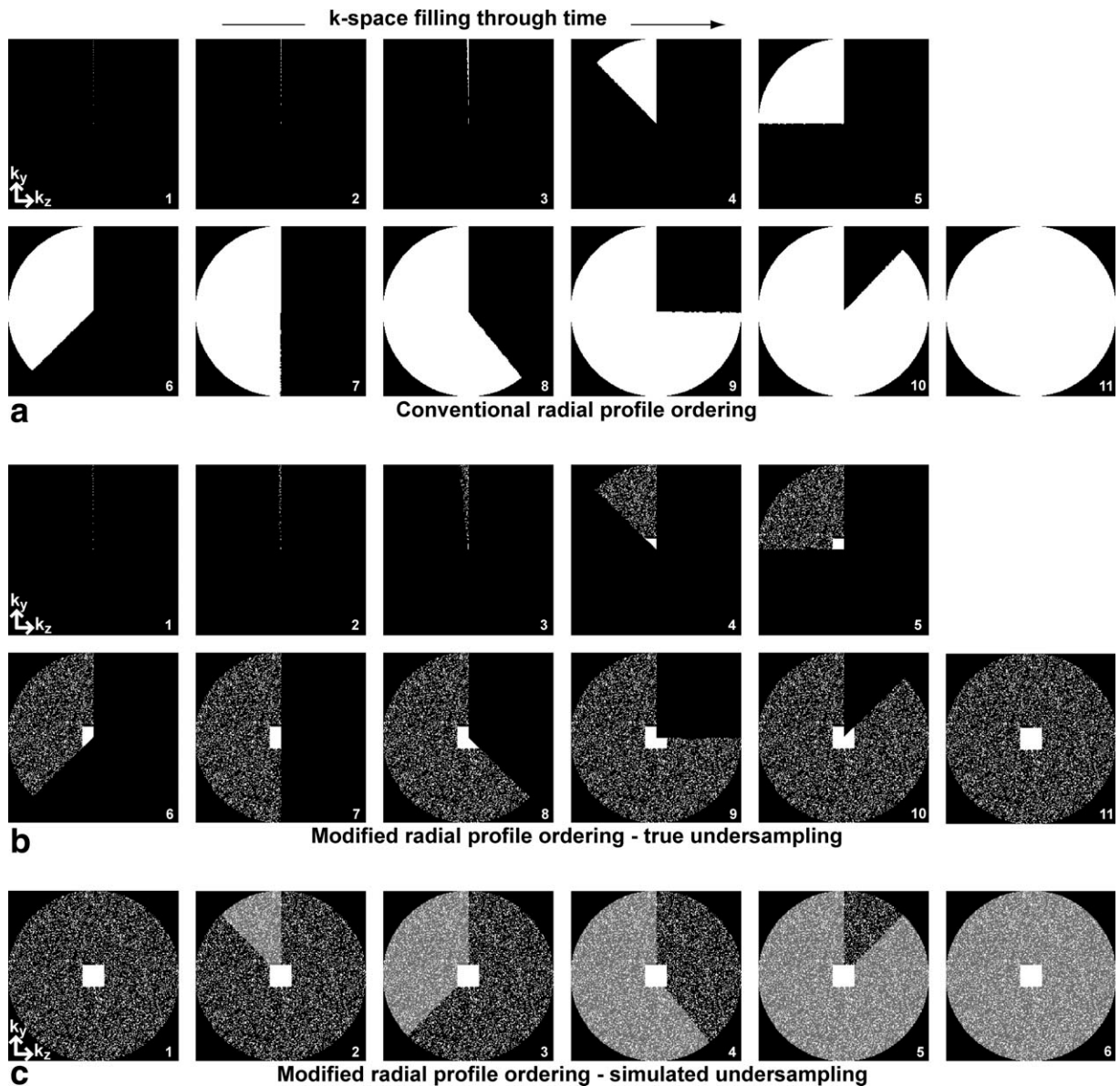


FIG. 1. Profile ordering in 3D-segmented acquisition through time for (a) conventional radial profile ordering for a fully sampled acquisition, (b) modified radial profile ordering with true undersampling (rate 4 is shown as an example), and (c) simulated undersampling. First, a subset of the fully sampled $k_y - k_z$ lines is selected randomly based on a given undersampling rate, while ensuring that the central $k_y - k_z$ region is included. Then, the selected $k_y - k_z$ lines are reordered in a radial fashion before the acquisition. For simulated undersampling, the data acquisition is continued after b11 (white dots represent the lines already acquired) to acquire the rest of the k -space lines (gray dots in c), such that the k -space is fully sampled (within an elliptical window) in (c6). In both (b) and (c), the acquisition of each shot starts from the closest point to the center and moves to the outer k -space.

coronary MRI, during which 0.2 mmol/kg Gd-BOPTA was injected intravenously using a bolus (2 mL/s) infusion. Approximately 2 min after the injection, during which the blood T1 value stabilizes [17], a Look-Locker sequence was performed to visually estimate the optimal inversion time (TI). A free-breathing electrocardiogram navigator-gated SSFP whole-heart coronary MRI sequence was used for acquisition. A nonselective inversion pulse with the optimal TI was used to suppress myocardial signal, and a fat-saturation sequence was used to improve contrast between the coronary arteries and the surrounding fat. The imaging parameters were TR/TE = 4.8/2.4 ms, flip angle = 90°, field of view =

$300 \times 300 \times 120 \text{ mm}^3$, and spatial resolution = $1.3 \times 1.3 \times 1.3 \text{ mm}^3$. The electrocardiogram delay was selected using a breath-held high-temporal resolution cine SSFP image before the coronary MRI, which was used to visually identify the quiescent period of the right coronary artery (RCA). A navigator placed on the dome of the right hemidiaphragm was used for respiratory motion compensation, using prospective real-time correction with a 5-mm end-expiration gating window and 0.6 superior-inferior tracking ratio [29,30]. The data acquisition was accelerated by a rate of 4 in $k_y - k_z$ using a pseudo-random pattern generation and the proposed radial profile ordering. Figure 2 depicts an incoherent

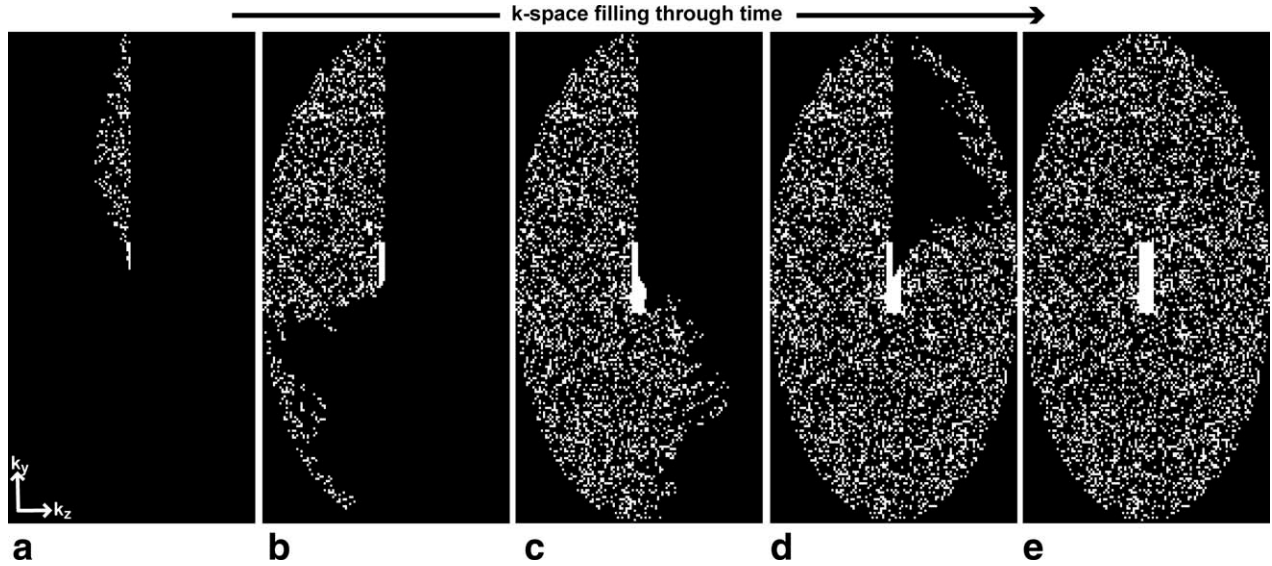


FIG. 2. a–e: Profile ordering in 3D segmented acquisition for one of the example patterns used in the prospectively undersampled acquisitions. The net acceleration rate is four with respect to the elliptical window, which corresponds to an acceleration rate of 5.1 for the whole k -space. Because of the mismatch between elliptical geometry as specified by different FOVs in y and z axes, and the radial profile ordering with the requirement of starting each shot from innermost k -space, some outer k -space lines are acquired earlier than the inner k -space lines corresponding to the same phase in the $k_y - k_z$ plane (e.g., lower left quadrant of [b] and upper right quadrant of [d]). This phenomenon applies to both the conventional and the modified radial profile ordering.

undersampling pattern used in one of the whole-heart coronary MRI acquisitions, and how the k -space was filled through time using the proposed modified radial profile ordering.

Patient Study

Four patients (two females, 55.0 ± 13.3 years) with suspected coronary artery disease were recruited. For two of these patients, 0.1 mmol/kg Gd-BOPTA was injected intravenously, and for one patient, 0.2 mmol/kg Gd-BOPTA was injected intravenously, using a bolus infusion for all patients. Isosorbide dinitrate was administered for two of these patients (with acceptable blood pressure). A lower dose of 0.1 mmol/kg of contrast agent was used for patients with estimated glomerular filtration rate value of less than $60 \text{ mL}/\text{min}/1.73 \text{ m}^2$. Contrast-enhanced coronary imaging was performed as described for the healthy subjects. For the patient studies, the data acquisition was accelerated by a rate of 3 in $k_y - k_z$ using a pseudo-random pattern generation and the proposed radial profile ordering. A more conservative acceleration rate was used for patients to ensure diagnostic quality of the images.

Image Reconstruction

The acquired raw data were exported from the scanner, and images were reconstructed offline using the LOST algorithm. A thorough comparison of LOST with existing CS methods has been reported elsewhere [26]. In summary, with LOST, an estimate of the image is used to adaptively identify 2D image blocks of similar signal content, which are grouped into similarity clusters. For each voxel of the image, the $N_b \times N_b$ reference block whose top left corner is at that voxel is compared using

the normalized l_2 distance to another block. If this distance is less than a threshold, λ_{match} , these blocks are declared to be similar, and the compared block is added to the similarity cluster of that voxel. Then, a 3D fast Fourier transform is applied to each similarity cluster to adaptively sparsify the data [26]. The algorithm then alternates between data consistency and shrinkage of the 3D fast Fourier transform coefficients of the similarity cluster.

LOST reconstruction was implemented in Matlab (v7.6, MathWorks, Natick, MA), with the adaptive learning and nonlinear shrinkage portions implemented in C++. The details of the implementation, as well as the reconstruction parameters, are described in the Appendix section. We note that the same reconstruction parameters were used in all cases, allowing for fully automated reconstructions. For all coronary MRI datasets, LOST reconstruction was performed for each coil independently using a parallel implementation on a central processing unit cluster, where five central processing units with 4 GB of memory were used for reconstructing each individual coil image. The reconstruction time was ~ 70 min. Comparison images with zero filling were also generated from the measured data, where the k -space lines that were not acquired were replaced with zero, and an inverse Fourier transform was applied for the zero-filled images. In all cases, the final images were generated by root-sum-squares of the individual coil images.

Image and Statistical Analysis

Subjective image scores and vessel length and sharpness measurements were used to evaluate the LOST and zero-filled reconstructions for all datasets. A qualitative assessment of coronary artery image quality was performed in

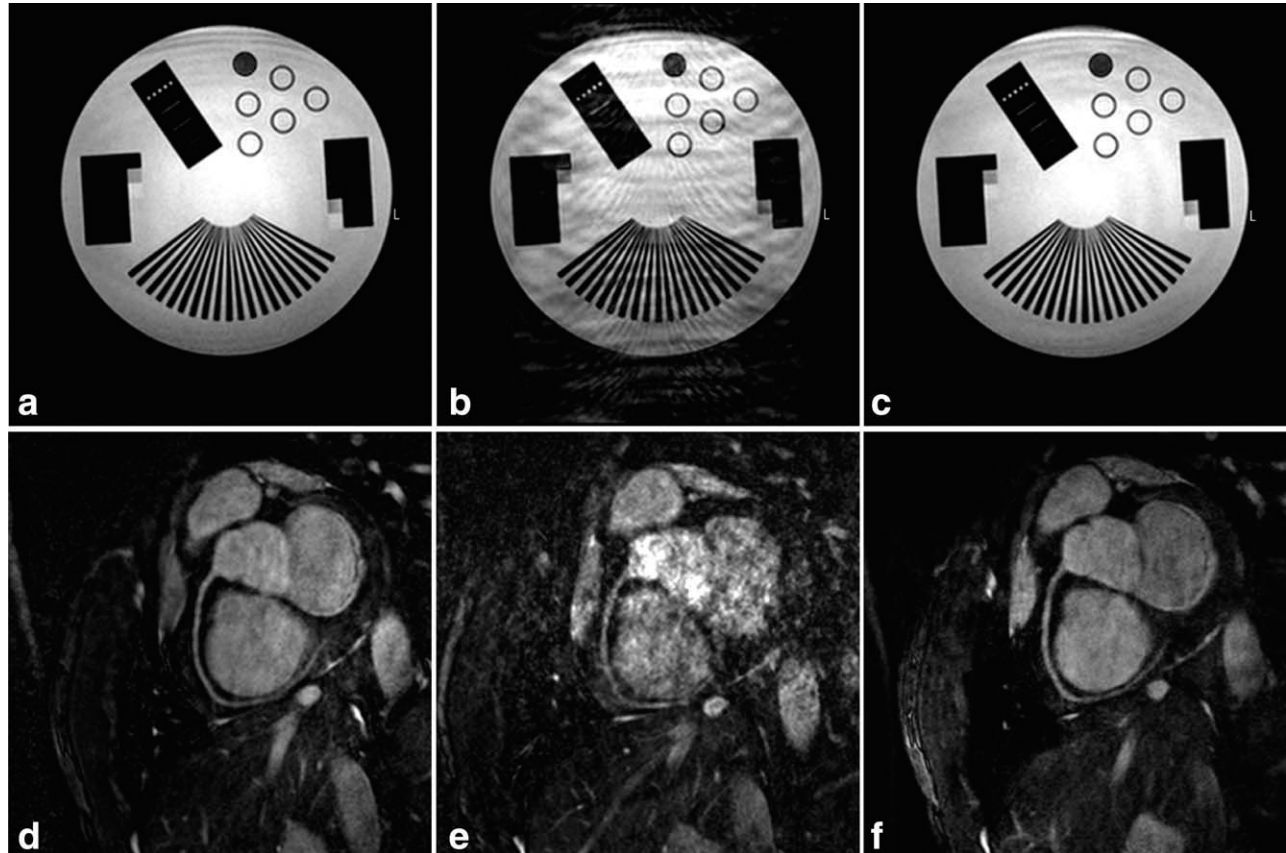


FIG. 3. Effects of different profile ordering schemes in phantom (top) and in vivo right coronary artery (RCA) imaging (bottom). (a, d) Fully sampled; (b, e) images acquired with simulated prospective random undersampling of rate two with no profile ordering. Artifacts are apparent in these images even though they are fully sampled; (c) depicts a phantom image acquired with the proposed profile ordering with a simulated prospective random undersampling; (f) depicts a true undersampling of rate two with the proposed profile ordering and a random undersampling pattern, reconstructed using LOST. The proposed ordering scheme mitigates artifacts associated with random undersampling patterns and improves visibly over no profile ordering.

consensus by two experienced independent blinded readers with coronary MRI experience based on the axial images from the 3D datasets, using a four-point scale system [31]: 1, poor or uninterpretable (coronary artery visible, with markedly blurred borders and edges); 2, fair (coronary artery visible, with moderately blurred borders and edges); 3, good (coronary artery visible, with mildly blurred borders and edges); 4, excellent (coronary artery visible, with sharply defined borders and edges). Separate scores were given for the proximal, mid, and distal segments of the RCA, the left anterior descending artery (LAD), and the left circumflex artery (LCX); and for the left main artery.

A SoapBubble tool [32] was used to quantitatively evaluate vessel sharpness for RCA, LAD, and LCX. Vessel sharpness scores were calculated for both sides of the vessel using a Deriche algorithm [33]. Final normalized sharpness was defined as the average score of both sides divided by the center of vessel intensity. The visualized length of RCA, LAD, and LCX was measured using the SoapBubble tool by following the coronary arteries through the axial sections sequentially.

Imaging scores, normalized vessel sharpness, and vessel length are presented as mean \pm one standard deviation. The signed rank test was used for imaging scores to

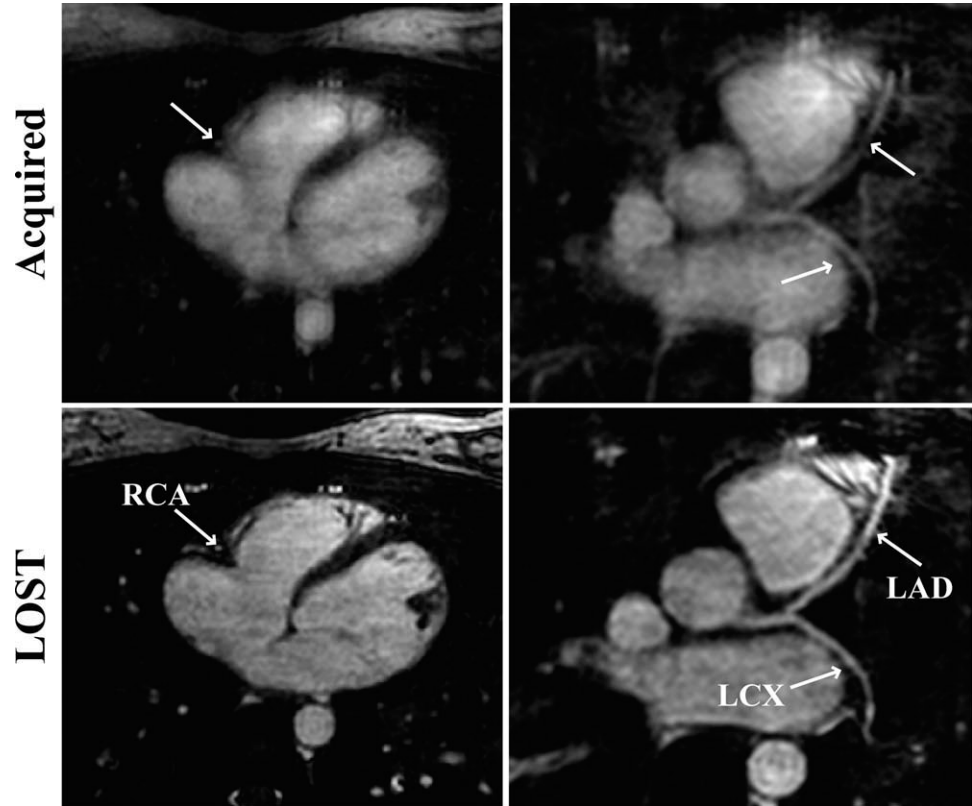
test for the null hypothesis that the central tendency of the difference was zero for the two reconstructions. All statistical analyses were performed using SAS (v9.3, SAS Institute, Cary, NC). The normalized sharpness scores and vessel length were compared using the paired *t*-test. A *P* value of <0.05 was considered to be significant.

RESULTS

Profile Ordering for Randomly Undersampled *k*-Space

Figure 3a–c shows the phantom results for the SSFP acquisitions, with a fully sampled reference acquisition using conventional radial profile ordering (3a), a fully sampled acquisition using simulated prospective undersampling with rate 2 and random profile ordering (3b), and a fully sampled acquisition using simulated prospective undersampling with rate 2 and the proposed modified radial profile ordering (3c). Even though a random undersampling pattern is used, there is noticeable artifact reduction when the proposed acquisition ordering is used (3c) instead of random ordering (3b). Figure 3d–f shows reformatted images from a targeted RCA MRI, with a fully sampled reference acquisition using conventional radial profile ordering (3d), a fully sampled acquisition using simulated prospective undersampling with

FIG. 4. An example axial slice (left) and reformatted axial image (right) depicting the left coronary system of a healthy subject using zero filling (acquired) and LOST reconstruction. The left coronaries are better defined (image scores 3.3 ± 0.7 for LAD and 3.4 ± 1.0 for LCX) in the LOST reconstruction, but are blurry in the original acquired images (image scores 1.2 ± 0.4 for LAD and 1.4 ± 0.6 for LCX) due to the high rate of undersampling (RCA, right coronary artery; LAD, left anterior descending, LCX, left circumflex).



rate 2 and random profile ordering (3e), and a true prospectively undersampled acquisition with acceleration rate 2 and the proposed modified radial profile ordering (3f). The LOST reconstruction for the true prospective random undersampling of rate 2, with the proposed acquisition ordering (3f), shows fewer artifacts and better image quality than the fully sampled data acquired with random acquisition ordering (3e). Finally, we note that among the two datasets acquired with the proposed profile ordering, the in vivo dataset in (3f) is 2-fold undersampled, whereas that of the phantom in (3c) is fully sampled. Hence the reconstruction for the in vivo dataset is more challenging, but the results are visually similar to the reference.

Contrast-Enhanced Whole-Heart Coronary MRI

Healthy Subject Study

Contrast-enhanced whole-heart coronary MRI was performed successfully in all subjects, without complications. The nominal scan time for these acquisitions was 2:50 min at 70 heart beats per min, assuming 100% navigator gating efficiency. The average scan time was $6:04 \pm 1:18$ min, with range between 4:31 and 8:15 min. The difference between the nominal scan time and the actual average scan time is due to the differences in breathing patterns and heart rates of the subjects.

Figure 4 depicts an example axial slice and a reformatted axial image from one of the acquisitions, showing the LAD and LCX of the subject, reconstructed with zero filling (acquired) as well as with LOST. LOST reconstruction removes the aliasing artifacts successfully, allowing for much improved definition compared to the zero-filled approach, including the distal segments. Fig-

ure 5 shows a sample axial slice and reformatted RCA image from another subject using both zero filling and LOST reconstruction. The improvement in visualization from using LOST is consistent across multiple slices, with improved definition of the RCA.

Table 1 depicts the qualitative assessment of the coronary MRI for LOST and zero-filled reconstructions. For the images reconstructed with LOST, all major coronary arteries were visualized in all subjects. In contrast, for the zero-filled images, RCA, LAD, and LCX were not visualized for one, two, and five subjects, respectively. LOST provides a statistically significant improvement over the zero-filled reconstruction for subjective image quality for all segments of all coronary arteries. Also notably, the average visualization score for LOST is close to an excellent value for each major artery. Table 2 depicts the vessel length and sharpness measurements for the two reconstructions. For the zero-filled images, where the arteries were not visualized, these measurements were omitted, and the averaging and statistical comparisons were performed over the measurements for the remaining subjects. The visualized length of the coronaries for LOST reconstructions is significantly longer for each major artery compared to the zero-filled images, which is consistent with the subjective image scores. Similarly, the normalized sharpness scores for LOST reconstructions were also significantly better than those of the zero-filled images.

Patient Study

Contrast-enhanced whole-heart coronary MRI was performed successfully in all patients, without complications. Figure 6 shows a reformatted axial image from

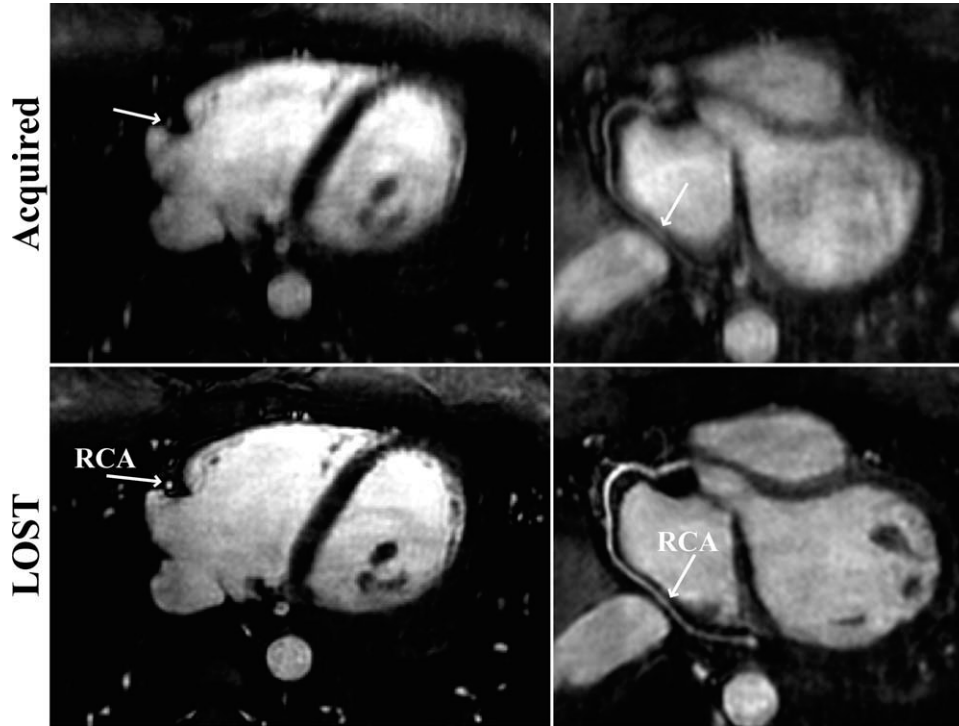


FIG. 5. An example axial slice (left) and reformatted axial image (right) depicting the right coronary artery (RCA) of another subject using zero filling (acquired) and LOST reconstruction. The LOST reconstruction allows better definitions (image score 3.7 ± 0.7 vs. 1.5 ± 0.5) of the RCA in the proximal, mid, and distal regions.

accelerated coronary MRI reconstructed using LOST, depicting the RCA of the patient, as well as a corresponding RCA image from invasive X-ray coronary angiography, which shows significant occlusion of the proximal RCA. Figure 7a,b shows axial slices from the LOST-reconstructed 3D whole-heart coronary MRI showing coronary stenosis in RCA and left coronary artery, respectively, in a 47-year-old male patient with coronary artery disease undergoing coronary artery bypass graft. Corresponding invasive X-ray coronary angiography (Fig. 7c,d) is in agreement with this finding.

DISCUSSION

In this study, we have demonstrated the efficacy of an accelerated contrast-enhanced whole-heart coronary MRI method using a prospective random undersampling scheme with profile ordering and the LOST reconstruction technique. These reconstruction and acquisition techniques allow for very high-quality visualization of all coronary branches, with 4-fold accelerated acquisitions using only five-channel coils. The techniques were also used on patients with 3-fold acceleration, generating diagnostic images.

Prospective random under sampling is a necessary condition for CS-based techniques. However, there has

been little attention on what order the random k -space samples must be acquired to minimize artifacts due to Eddy currents and flow. Much work on CS has been based on retrospective undersampling of fully sampled data, which fails to capture realistic scenarios, for instance, when contrast agents have been used. Previous work that involves 3D acquisitions with prospective undersampling has used GRE sequences [25,34], which are less susceptible to Eddy current artifacts than SSFP sequences [27]. Our study indicates that special care must be given to profile ordering in order to mitigate artifacts due to randomness of the undersampling pattern. The proposed radial ordering scheme is effective in mitigating these artifacts by reducing gradient switching.

We also note that noncontrast enhanced targeted coronary MRI was used in our pilot study instead of contrast-enhanced whole-heart coronary MRI, which is the focus of this work. The goal of the pilot study on profile ordering was to devise a profile-ordering scheme that mitigates artifacts due to the random undersampling pattern for 3D acquisitions. Thus, a repeatable acquisition, not affected by contrast wash-out, which can be fully acquired within 10 min, was needed to test multiple different techniques. Because a fully sampled whole-heart scan takes about ~ 25 min, it would have been very

Table 1

Comparison of Average Subjective Imaging Scores (1 = Poor, 2 = Fair, 3 = Good, 4 = Excellent) Between Zero-Filled and LOST Reconstructions

| | RCA | LAD | LCX | RCA | LAD | LCX | RCA | LAD | LCX | LM | OVERALL |
|-----------------|---------------|---------------|---------------|---------------|---------------|---------------|---------------|---------------|---------------|---------------|---------------|
| Zero filled | 1.9 ± 0.3 | 1.2 ± 0.4 | 1.6 ± 0.7 | 1.3 ± 0.5 | 1.3 ± 0.5 | 1.4 ± 0.7 | 1.2 ± 0.4 | 1.2 ± 0.4 | 1.3 ± 0.5 | 1.3 ± 0.5 | 1.2 ± 0.4 |
| LOST | 3.8 ± 0.6 | 3.7 ± 0.5 | 3.9 ± 0.3 | 3.6 ± 0.7 | 3.1 ± 0.7 | 3.2 ± 1.0 | 3.6 ± 0.7 | 3.2 ± 0.6 | 3.0 ± 1.2 | 3.7 ± 0.5 | 3.6 ± 0.5 |
| <i>P</i> -value | 0.002 | 0.002 | 0.002 | 0.002 | 0.004 | 0.004 | 0.002 | 0.002 | 0.008 | 0.002 | 0.002 |

LOST was evaluated significantly better for all sections of all arteries (RCA, right coronary artery; LAD, left anterior descending; LCX, left circumflex; LM, left main). A *P*-value less than 0.05 is considered significant.

Table 2
Vessel Length and Normalized Sharpness Measurements (Higher Is Better) for Zero-Filled and LOST Reconstructions

| | Vessel length (mm) | | | Normalized vessel sharpness | | |
|-----------------|--------------------|-------------|-------------|-----------------------------|-------------|-------------|
| | RCA | LAD | LCX | RCA | LAD | LCX |
| Zero filled | 93.4 ± 28.0 | 53.8 ± 22.6 | 50.5 ± 12.6 | 0.43 ± 0.11 | 0.36 ± 0.11 | 0.37 ± 0.03 |
| LOST | 129.8 ± 13.2 | 94.7 ± 18.7 | 67.9 ± 9.1 | 0.64 ± 0.05 | 0.54 ± 0.07 | 0.48 ± 0.05 |
| <i>P</i> -value | 0.001 | 0.0001 | 0.083 | <0.0001 | 0.007 | 0.035 |

LOST is significantly better for all vessels. Zero-filled length measurements were not possible for the RCA of 1 subject, LAD of 2 subjects, and LCX of 5 subjects; therefore, these subjects were excluded in the measurements and subsequent analysis. Furthermore, zero-filled sharpness measurements were not available for the LAD and LCX of two additional subjects, which were also excluded. A *P*-value less than 0.05 is considered significant.

difficult to get images of high quality during such long scans, which would make it difficult to establish whether any observed artifacts were due to the random undersampling and/or ordering or due to the inferior quality of images acquired in such a long scan. Finally, we emphasize that we did not aim to study profile ordering to maximize the benefits of contrast agents, but focused on minimizing the artifacts due to random undersampling patterns. Further improvements may be possible by using additional constraints specific to the presence of the contrast agents in designing the profile ordering, but this is beyond the scope of our pilot study.

LOST reconstruction offers an acceleration technique that does not exclusively rely on the number of coil elements. This is in contrast to parallel-imaging techniques, such as sensitivity encoding or generalized autocalibrating partially parallel acquisition. Acceleration rates reported in previous studies on contrast-enhanced coronary MRI with 5–16 channel-coil arrays have been limited to 2-fold with these techniques [16–18,20], whereas LOST is able to achieve a 4-fold acceleration with only a five-channel cardiac coil. Although we have not provided a comparison with these parallel-imaging methods [35–37], it is not anticipated that these techniques can offer a similar acceleration rate with five-channel coils. The main difficulty in providing such a comparison is that the sampling schemes used by these methods and

our method are conflicting. The former techniques require uniform undersampling for high performance, while LOST and other CS-based techniques require random Cartesian sampling. Although it is possible to use conjugate-gradient-type methods with parallel imaging [25,38], this results in performance deterioration and would result in an unfavorable advantage for our method. Because our coronary MRI protocol requires contrast enhancement, it is also not feasible to do a follow-up scan with alternate sampling.

The contrast agent in this study was beneficial in several ways. Bolus infusion of Gd-BOPTA leads to a higher SNR and CNR compared to non-contrast-enhanced coronary MRI [17]. Thus, although SNR loss may be incurred due to accelerated imaging, the starting SNR and CNR are higher. Second, when a contrast agent is used, most of the energy of the *k*-space is highly concentrated in the center of *k*-space, which is fully sampled in the prospective random undersampling scheme. This proves to be beneficial for LOST reconstruction, and an acceleration rate of 4 can be used reliably, which is an improvement in acceleration rate from the non-contrast-enhanced targeted coronary MRI reported previously [26].

In this study, LOST reconstruction was performed individually for each coil. Hence, the reconstruction process was parallelized over each coil in a straightforward manner to reduce the reconstruction time by 5-fold.

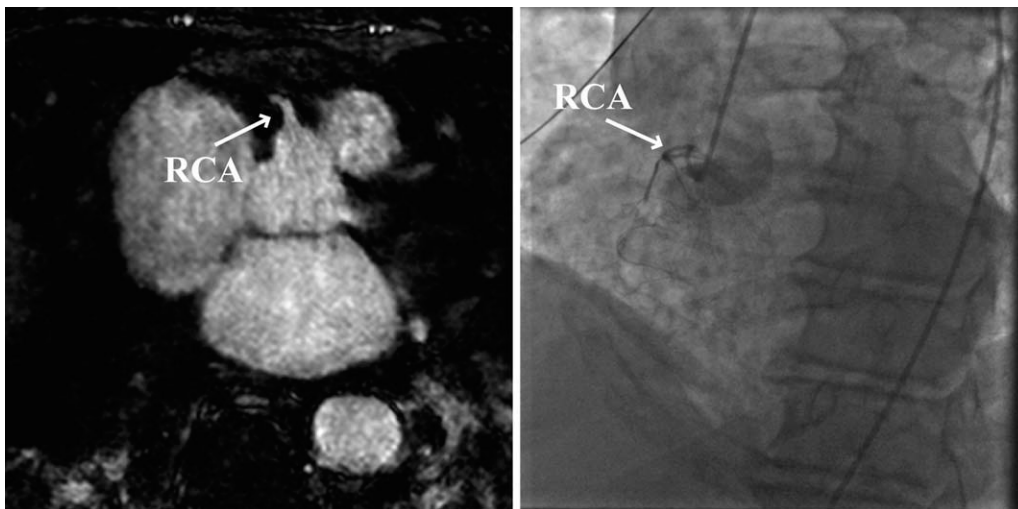


FIG. 6. Reformatted LOST-reconstructed coronary MRI (left) showing occlusion of the right coronary artery (RCA). The X-ray angiography images (right) confirm this finding.

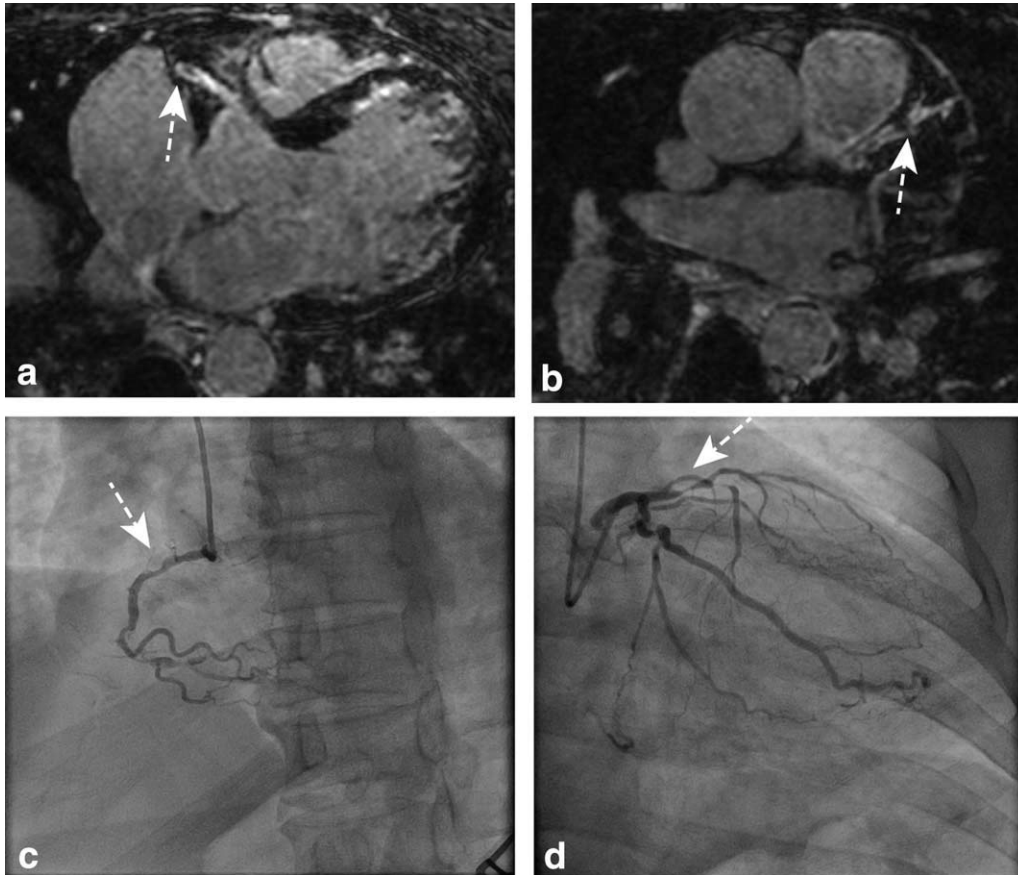


FIG. 7. Two axial slices from the LOST-reconstructed 3D whole-heart coronary MRI showing coronary stenosis in (a) right coronary artery and (b) left coronary artery with (c, d) corresponding invasive X-ray coronary angiography in a 47-year-old male patient with coronary artery disease undergoing coronary artery bypass graft.

However, the reconstruction time is still too long to be clinically feasible. Further parallelization is required, especially during the adaptive identification of similarity clusters, which is the most computationally intensive part of the algorithm.

Our study has several limitations. Only a small number of healthy adult subjects and patients were studied. Further studies are needed to study the clinical evaluation of this approach in a larger cohort with known or suspected coronary artery disease. Additionally, we have not provided SNR/CNR measurements comparing the two reconstructions. The difficulty with these measurements is that the reconstruction algorithms inherently threshold and shrink the noise in the nonsignal areas. Hence, the measurement noise level cannot be reliably determined from the final reconstructed image. We did not combine parallel imaging with CS reconstruction as reported in [25,34,39,40] due to unavailability of a phased-array coil with a higher number of elements. Our pilot study using five-element phased array coil did not show noticeable improvements in image quality or acceleration rate when using both techniques simultaneously.

CONCLUSION

We have demonstrated that LOST reconstruction can be used to accelerate contrast-enhanced whole-heart coro-

nary MRI by a factor of 4 using a clinically available five-channel phased-array coil. Future studies examining the clinical utility of this approach are warranted.

APPENDIX

Implementation Details of LOST

The LOST algorithm was implemented in two stages as described in [26]. For the first stage, a low-resolution image generated from fully sampled central k -space was used for identification of similarity clusters, with parameters $N_b = 8$ and $\lambda_{\text{match}} = 0.1$. For each reference block, comparison with other blocks was limited to a neighborhood of radius 8 in x - y and of radius 1 in z direction. The maximum number of blocks in a similarity cluster was limited to 16. For shrinkage in the first stage, hard thresholding was used, with thresholding parameter τ_{ht} was set to 0.05 times the largest (in absolute value) coefficient of the zero-filled coil image. For the second stage, the estimate from the first stage was used for the identification of similarity clusters with parameters $N_b = 4$ and $\lambda_{\text{match}} = 0.05$ and the same remaining parameters from the first stage. For shrinkage, LOST alternated between hard thresholding and Wiener filtering, with thresholding parameters τ_{ht} and τ_{wie} respectively set to 0.04 and 0.03 times the largest coefficient of the estimate from the first stage.

REFERENCES

- Brittain JH, Hu BS, Wright GA, Meyer CH, Macovski A, Nishimura DG. Coronary angiography with magnetization-prepared T2 contrast. *Magn Reson Med* 1995;33:689–696.
- Botnar RM, Stuber M, Danias PG, Kissinger KV, Manning WJ. Improved coronary artery definition with T2-weighted, free-breathing, three-dimensional coronary MRA. *Circulation* 1999;99:3139–3148.
- Meyer CH, Hu BS, Nishimura DG, Macovski A. Fast spiral coronary artery imaging. *Magn Reson Med* 1992;28:202–213.
- Bhat H, Ge L, Nielles-Vallespin S, Zuehlsdorff S, Li D. 3D radial sampling and 3D affine transform-based respiratory motion correction technique for free-breathing whole-heart coronary MRA with 100% imaging efficiency. *Magn Reson Med* 2011;65:1269–1277.
- Hu P, Chuang ML, Ngo LH, Stoeck CT, Peters DC, Kissinger KV, Goddu B, Goepfert LA, Manning WJ, Nezafat R. Coronary MR imaging: effect of timing and dose of isosorbide dinitrate administration. *Radiology* 2010;254:401–409.
- Nezafat R, Ouwerkerk R, Derbyshire AJ, Stuber M, McVeigh ER. Spectrally selective B1-insensitive T2 magnetization preparation sequence. *Magn Reson Med* 2009;61:1326–1335.
- van Elderen SG, Versluis MJ, Westenberg JJ, Agarwal H, Smith NB, Stuber M, de Roos A, Webb AG. Right coronary MR angiography at 7 T: a direct quantitative and qualitative comparison with 3 T in young healthy volunteers. *Radiology* 2010;257:254–259.
- Gharib AM, Abd-Elmoniem KZ, Herzka DA, Ho VB, Locklin J, Tzatha E, Stuber M, Pettigrew RI. Optimization of coronary whole-heart MRA free-breathing technique at 3 Tesla. *Magn Reson Imaging* 2011;29:1125–1130.
- Knuesel PR, Nanz D, Wolfensberger U, Saranathan M, Lehning A, Luescher TF, Marincek B, von Schulthess GK, Schwitler J. Multislice breath-hold spiral magnetic resonance coronary angiography in patients with coronary artery disease: effect of intravascular contrast medium. *J Magn Reson Imaging* 2002;16:660–667.
- Paetsch I, Jahnke C, Barkhausen J, Spuentrup E, Cavagna F, Schnackenburg B, Huber M, Stuber M, Fleck E, Nagel E. Detection of coronary stenoses with contrast enhanced, three-dimensional free breathing coronary MR angiography using the gadolinium-based intravascular contrast agent gadocoletic acid (B-22956). *J Cardiovasc Magn Reson* 2006;8:509–516.
- Prompona M, Cyran C, Nikolaou K, Bauner K, Reiser M, Huber A. Contrast-enhanced whole-heart MR coronary angiography at 3.0 T using the intravascular contrast agent gadofosveset. *Invest Radiol* 2009;44:369–374.
- Goldfarb JW, Edelman RR. Coronary arteries: breath-hold, gadolinium-enhanced, three-dimensional MR angiography. *Radiology* 1998;206:830–834.
- Zheng J, Bae KT, Woodard PK, Haacke EM, Li D. Efficacy of slow infusion of gadolinium contrast agent in three-dimensional MR coronary artery imaging. *J Magn Reson Imaging* 1999;10:800–805.
- Li D, Carr JC, Shea SM, Zheng J, Deshpande VS, Wielopolski PA, Finn JP. Coronary arteries: magnetization-prepared contrast-enhanced three-dimensional volume-targeted breath-hold MR angiography. *Radiology* 2001;219:270–277.
- Weber OM, Martin AJ, Higgins CB. Whole-heart steady-state free precession coronary artery magnetic resonance angiography. *Magn Reson Med* 2003;50:1223–1228.
- Bi X, Carr JC, Li D. Whole-heart coronary magnetic resonance angiography at 3 Tesla in 5 minutes with slow infusion of Gd-BOPTA, a high-relaxivity clinical contrast agent. *Magn Reson Med* 2007;58:1–7.
- Hu P, Chan J, Ngo LH, Smink J, Goddu B, Kissinger KV, Goepfert L, Hauser TH, Rofsky NM, Manning WJ, Nezafat R. Contrast-enhanced whole-heart coronary MRI with bolus infusion of gadobenate dimeglumine at 1.5 T. *Magn Reson Med* 2011;65:392–398.
- Yang Q, Li K, Liu X, Bi X, Liu Z, An J, Zhang A, Jerecic R, Li D. Contrast-enhanced whole-heart coronary magnetic resonance angiography at 3.0-T: a comparative study with X-ray angiography in a single center. *J Am Coll Cardiol* 2009;54:69–76.
- Bhat H, Yang Q, Zuehlsdorff S, Li K, Li D. Contrast-enhanced whole-heart coronary magnetic resonance angiography at 3 T with radial EPI. *Magn Reson Med* 2011;66:82–91.
- Tang L, Merkle N, Schar M, Korosoglou G, Solaiyappan M, Hombach V, Stuber M. Volume-targeted and whole-heart coronary magnetic resonance angiography using an intravascular contrast agent. *J Magn Reson Imaging* 2009;30:1191–1196.
- Nagata M, Kato S, Kitagawa K, Ishida N, Nakajima H, Nakamori S, Ishida M, Miyahara M, Ito M, Sakuma H. Diagnostic accuracy of 1.5-T unenhanced whole-heart coronary MR angiography performed with 32-channel cardiac coils: initial single-center experience. *Radiology* 2011;259:384–392.
- Niendorf T, Hardy CJ, Giaquinto RO, Gross P, Cline HE, Zhu Y, Kenwood G, Cohen S, Grant AK, Joshi S, Rofsky NM, Sodickson DK. Toward single breath-hold whole-heart coverage coronary MRA using highly accelerated parallel imaging with a 32-channel MR system. *Magn Reson Med* 2006;56:167–176.
- Block KT, Uecker M, Frahm J. Undersampled radial MRI with multiple coils. Iterative image reconstruction using a total variation constraint. *Magn Reson Med* 2007;57:1086–1098.
- Lustig M, Donoho DL, Pauly JM. Sparse MRI: the application of compressed sensing for rapid MR imaging. *Magn Reson Med* 2007;58:1182–1195.
- Vasanawala SS, Alley MT, Hargreaves BA, Barth RA, Pauly JM, Lustig M. Improved pediatric MR imaging with compressed sensing. *Radiology* 2010;256:607–616.
- Akcakaya M, Basha TA, Goddu B, Goepfert LA, Kissinger KV, Tarokh V, Manning WJ, Nezafat R. Low-dimensional-structure self-learning and thresholding: regularization beyond compressed sensing for MRI reconstruction. *Magn Reson Med* 2011;66:756–767.
- Bieri O, Markl M, Scheffler K. Analysis and compensation of eddy currents in balanced SSFP. *Magn Reson Med* 2005;54:129–137.
- Stuber M, Botnar RM, Danias PG, Sodickson DK, Kissinger KV, Van Cauteren M, De Becker J, Manning WJ. Double-oblique free-breathing high resolution three-dimensional coronary magnetic resonance angiography. *J Am Coll Cardiol* 1999;34:524–531.
- Wang Y, Riederer SJ, Ehman RL. Respiratory motion of the heart: kinematics and the implications for the spatial resolution in coronary imaging. *Magn Reson Med* 1995;33:713–719.
- Danias PG, Stuber M, Botnar RM, Kissinger KV, Edelman RR, Manning WJ. Relationship between motion of coronary arteries and diaphragm during free breathing: lessons from real-time MR imaging. *AJR Am J Roentgenol* 1999;172:1061–1065.
- Kim WY, Danias PG, Stuber M, Flamm SD, Plein S, Nagel E, Langerak SE, Weber OM, Pedersen EM, Schmidt M, Botnar RM, Manning WJ. Coronary magnetic resonance angiography for the detection of coronary stenoses. *N Engl J Med* 2001;345:1863–1869.
- Etienne A, Botnar RM, Van Muiswinkel AM, Boesiger P, Manning WJ, Stuber M. “Soap-Bubble” visualization and quantitative analysis of 3D coronary magnetic resonance angiograms. *Magn Reson Med* 2002;48:658–666.
- Deriche R. Fast algorithms for low-level vision. *IEEE Trans Pattern Anal Mach Intell* 1990;12:78–87.
- Otazo R, Xu J, Axel L, Sodickson D. Combination of compressed sensing and parallel imaging for highly-accelerated 3D first-pass cardiac perfusion MRI. In: Proceedings of the 18th Scientific Meeting of ISMRM, Stockholm, 2010 May. p 344.
- Sodickson DK, Manning WJ. Simultaneous acquisition of spatial harmonics (SMASH): fast imaging with radiofrequency coil arrays. *Magn Reson Med* 1997;38:591–603.
- Pruessmann KP, Weiger M, Scheidegger MB, Boesiger P. SENSE: sensitivity encoding for fast MRI. *Magn Reson Med* 1999;42:952–962.
- Griswold MA, Jakob PM, Heidemann RM, Nittka M, Jellus V, Wang J, Kiefer B, Haase A. Generalized autocalibrating partially parallel acquisitions (GRAPPA). *Magn Reson Med* 2002;47:1202–1210.
- Pruessmann KP, Weiger M, Bornert P, Boesiger P. Advances in sensitivity encoding with arbitrary k-space trajectories. *Magn Reson Med* 2001;46:638–651.
- Lustig M, Pauly JM. SPIRiT: iterative self-consistent parallel imaging reconstruction from arbitrary k-space. *Magn Reson Med* 2010;64:457–471.
- Akcakaya M, Nam S, Hu P, Moghari MH, Ngo LH, Tarokh V, Manning WJ, Nezafat R. Compressed sensing with wavelet domain dependencies for coronary MRI: a retrospective study. *IEEE Trans Med Imaging* 2011;30:1090–1099.